Inorg. Chem. **2009**, *48*, 1649−1654

Large Cation−Anion Materials Based on Trinuclear Ruthenium(III) Salts of Keggin and Wells-Dawson Anions Having Water-Filled Channels

Masooma Ibrahim, Michael H. Dickman, Andreas Suchopar, and Ulrich Kortz*

Jacobs University, School of Engineering and Science, P.O. Box 750 561, 28725 Bremen, Germany

Received November 1, 2008

Reaction of the trinuclear ruthenium(III) cation $[Ru_3O(OOCCH_3)_6(CH_3OH)_3]^+$ with the Keggin-type $[\alpha\text{-}GeW_{11}O_{39}]^{8-}$, $[\alpha\text{-}SiW_{11}O_{39}]^{8-}$, and $[\alpha\text{-}SiMo_{12}O_{40}]^{4-}$ and the Wells−Dawson-type $[\alpha\text{-}P_2W_{18}O_{62}]^{6-}$ polyanions in an aqueous, acidic medium resulted in plenary polyoxometalate-based materials $K_2Na[Ru_3O(OOCCH_3)_6(H_2O)_3][\alpha\text{-}GeW_{12}O_{40}]\cdot 10H_2O$ (**1**), $K_3[Ru_3O(OOCCH_3)_6(H_2O)_3][\alpha\text{-}SiW_{12}O_{40}]\cdot 18H_2O$ (**2**), $K_3[Ru_3O(OOCCH_3)_6(H_2O)_3][\alpha\text{-}SiMo_{12}O_{40}]\cdot 7H_2O$ (**3**), and $K_2Na[Ru_3O(OOCCH_3)_6(H_2O)_3]_3[\alpha\text{-}P_2W_{18}O_{62}]\cdot 26H_2O$ (**4**), respectively. All four materials, **1**−**4**, crystallize as sodium and/or potassium salts in the monoclinic space group $P2_1/n$. Compounds **1**−**4** were characterized by IR, thermogravimetric analysis, and single-crystal/powder X-ray diffraction (XRD). The isolated solid-state frameworks, composed of cocrystallized trinuclear ruthenium cations and polyanions, exhibit nanosized voids filled with crystal waters. These water molecules can be removed reversibly upon heating under a vacuum, and powder XRD measurements demonstrated that the crystallinity of the compound was preserved. Sorption studies on ethanol and methanol were also performed.

Introduction

Polyoxometalates (POMs) are discrete molecular metal−oxygen clusters of group 5 or 6 metals in high oxidation states (e.g., W^{VI}, Mo^{VI}, V^{V}).[1] POMs have potential applications in many diverse fields including catalysis, magnetism, medicine, materials science, and chemical analysis.[2] POMs are also suitable building blocks for crystalline, microstructured materials with unique physical and chemical properties.[3] The construction of inorganic or hybrid organic/inorganic nanostructured compounds with well-defined pores can exhibit a shape- or size-selective sorption of small organic molecules, leading to applications in separation science and catalytic processes.[4]

Recently, Mizuno and co-workers published a series of papers on the synthesis, structure, and selective sorption/catalysis properties of solid-state materials resulting from interaction of the oxo-centered chromium trimer cation $[Cr_3O(OOCH)_6(H_2O)_3]^+$ with Keggin polyanions.[5]

Due to the interesting redox, electrochemical, and catalytic properties of ruthenium, we decided to study the formation of ionic crystals made up of polyanions and the trinuclear, oxo-centered ruthenium(III) cation $[Ru_3O(OOCCH_3)_6(CH_3OH)_3]^+$, which was synthesized using the reported procedure of Meyer and co-workers.[6] Previous studies on $[Ru_3O(OOCCH_3)_6(CH_3OH)_3]^+$ indicate that it is an efficient catalyst for the selective oxidation of primary and secondary alcohols to aldehydes and ketones, using molecular oxygen

* To whom correspondence should be addressed. Fax: +49-(0)421-200-3229. E-mail: u.kortz@jacobs-university.de.

(1) (a) Pope, M. T.; Müller, A. *Angew. Chem., Int. Ed. Engl.* **1991**, *30*, 34. (b) Pope, M. T. *Comp. Coord. Chem. II* **2003**, *4*, 635.

(2) (a) *Chem. Rev* **1998**, *98*, 1−389 (Special Thematic Issue on Polyoxometalates). (b) Hill, C. L. *Comp. Coord. Chem. II* **2003**, *4*, 679. (c) *Polyoxometalate Molecular Science*; Borrás-Almenar, J. J., Coronado, E., Müller, A., Pope, M. T., Eds.; Kluwer: Dordrecht, The Netherlands, 2004.

(3) (a) Hölscher, M.; Englert, U.; Zibrowius, B.; Hölderich, W. F. *Angew. Chem., Int. Ed. Engl.* **1994**, *33*, 2491. (b) Müller, A.; Krickemeyer, E.; Bögge, H.; Schmidtmann, M.; Peters, F.; Menke, C.; Meyer, J. *Angew. Chem., Int. Ed.* **1997**, *36*, 484. (c) Khan, M. I.; Yohannes, E.; Powell, D. *Inorg. Chem.* **1999**, *38*, 212. (d) Hagrman, D.; Hagrman, P. J.; Zubieta, J. *Angew. Chem., Int. Ed.* **1999**, *38*, 3165. (e) Son, J. H.; Choi, H.; Kwon, Y. U. *J. Am. Chem. Soc.* **2000**, *122*, 7432.

(4) (a) Yaghi, O. M.; Guangming, L.; Hailian, L. *Nature* **1995**, *378*, 703. (b) Yoshinaga, Y.; Seki, K.; Nakato, T.; Okuhara, T. *Angew. Chem., Int. Ed.* **1997**, *36*, 2833. (c) Seo, J. S.; Whang, D.; Lee, H.; Jun, S. I.; Oh, J.; Jeon, Y. J.; Kim, K. *Nature* **2000**, *404*, 982. (d) Moulton, B.; Zaworotko, M. J. *Chem. Rev.* **2001**, *101*, 1629.

(5) (a) Uchida, S.; Hashimoto, M.; Mizuno, N. *Angew. Chem., Int. Ed.* **2002**, *41*, 2814. (b) Uchida, S.; Hashimoto, M.; Mizuno, N. *Chem.—Eur. J.* **2003**, *9*, 5850. (c) Uchida, S.; Mizuno, N. *J. Am. Chem. Soc.* **2004**, *126*, 1602. (d) Uchida, S.; Kawamoto, R.; Akatsuka, T.; Hikichi, S.; Mizuno, N. *Chem. Mater.* **2005**, *17*, 1367. (e) Lesbani, A.; Kawamoto, R.; Uchida, S.; Mizuno, N. *Inorg. Chem.* **2008**, *47*, 3349.

(6) Baumann, B. J.; Salmon, D. J.; Wilson, S. T.; Meyer, T. J.; Hatfield, W. E. *Inorg. Chem.* **1978**, *17*, 3342.

10.1021/ic802096v CCC: $40.75
Published on Web 01/21/2009

as the oxidant.[7] Transition-metal cluster complexes showing multielectron redox behavior are rare and usually not stable over wide ranges of oxidation states. On the other hand, complexes of the type $[Ru^{III}_3O(CO_2R)_6L_3]^+$ provide a unique opportunity to construct stable multimetal/multielectron/multistep redox systems. This behavior is important in the sense that it can be used as an artificial model in understanding the mechanisms of biological metalloenzymes.[6,8]

Herein, we report the synthesis and characterization of four solid-state materials based on the trinuclear ruthenium-monocation and Keggin- or Wells−Dawson-type polyanions.

Experimental Section

Materials and Methods. The precursor polyanions $[\alpha\text{-}GeW_{11}O_{39}]^{8-}$, $[\alpha\text{-}SiW_{11}O_{39}]^{8-}$, $[\alpha\text{-}SiMo_{12}O_{40}]^{4-}$, and $[\alpha\text{-}P_2W_{18}O_{62}]^{6-}$ were all synthesized according to published procedures, and their purity was checked with IR spectroscopy.[9] All other reagents were used as purchased without further purification.

Synthesis of $K_2Na[Ru_3O(OOCCH_3)_6(H_2O)_3][\alpha\text{-}GeW_{12}O_{40}]\cdot 10H_2O$ (1). To 20 mL of distilled water was added 2.5 mL (0.100 mmol) of $[Ru_3O(OOCCH_3)_6(CH_3OH)_3](OOCCH_3)$. After complete dissolution, 0.323 g (0.100 mmol) of $K_6Na_2[\alpha\text{-}GeW_{11}O_{39}]\cdot 13H_2O$ was added. Then, the pH was adjusted to 2.0 through the dropwise addition of 1 M HCl_{aq}. The solution was then stirred for 30 min at 50 °C, cooled to room temperature, and filtered. Slow evaporation of the solvent in an open vial at room temperature resulted in dark green crystals of **1** (yield 0.061 g, 14%) after ∼2 weeks. IR data for **1** in cm^{-1}: 1619(w), 1427(m), 1353(w), 975(s), 890(s), 828(w), 779(s), 687(w), 617(w), 532(w), 463(m). Elem. anal. calcd (found) for **KNa-1**: K, 2.0 (3.2); Na, 0.6 (0.88); Ge, 1.9 (1.4); Ru, 7.7 (7.6); W, 56.2 (59.4).

Synthesis of $K_3[Ru_3O(OOCCH_3)_6(H_2O)_3][\alpha\text{-}SiW_{12}O_{40}]\cdot 18H_2O$ (2) and $K_3[Ru_3O(OOCCH_3)_6(H_2O)_3][\alpha\text{-}SiMo_{12}O_{40}]\cdot 7H_2O$ (3). The synthetic procedures for compounds **2** and **3** are identical to that of **1**, but 0.322 g (0.100 mmol) of $K_8[\alpha\text{-}SiW_{11}O_{39}]\cdot 13H_2O$ and 0.203 g of $K_4[\alpha\text{-}SiMo_{12}O_{40}]\cdot 3H_2O$ were used, respectively. Dark green crystals of **2** (yield 0.044 g, 11%) and **3** (yield 0.100 g, 35%), respectively, were obtained after ∼2 weeks. IR data for **2** in cm^{-1}: 1625(m), 1420(m), 1353(w), 1018(w), 976(m), 923(s), 880(sh), 796(s), 686(w), 660(sh), 650(w), 531(w). Elem. anal. calcd (found) for **2**: Si, 0.7 (1.5); Ru, 7.5 (6.9); W, 54.6 (55.4). IR data for **3** in cm^{-1}: 1617(w), 1424(m), 1353(w), 958(w), 907(s), 791(s), 686(w), 617(w), 534(w). Elem. anal. calcd (found) for **3**: K, 4.2 (5.1); Si, 1.0 (1.9); Ru, 10.9 (11.5); Mo, 41.3 (41.5).

Synthesis of $K_2Na[Ru_3O(OOCCH_3)_6(H_2O)_3]_3[\alpha\text{-}P_2W_{18}O_{62}]\cdot 26H_2O$ (4). Compound **4** was synthesized by dissolving 7.5 mL (ca. 0.300 mmol) of $[Ru_3O(OOCCH_3)_6(CH_3OH)_3](OOCCH_3)$ in 20 mL of 0.01 M $HNO_{3(aq)}$ followed by 1.0 g (0.210 mmol) of $(NH_4)_6[\alpha\text{-}P_2W_{18}O_{62}]\cdot 14H_2O$. The solution was stirred at 50 °C for 30 min, cooled to room temperature, and then filtered. The filtrate was layered with a few drops of 1 M KCl. Slow evaporation of the solvent in an open vial at room temperature resulted in dark green crystals of **4** (yield 0.094 g, 13%) after ∼2 weeks. Compound **4** contains one sodium ion, although no such ions were explicitly used during the synthesis. Hence, it appears that the impurity results from residual sodium ions in the POM precursor. IR data for **4** in cm^{-1}: 1638(w), 1617(w), 1427(s), 1353(w), 1092(s), 960(s), 910(m), 795(s), 687(w), 619(w), 474(w) cm^{-1}. Elem. anal. calcd (found) for **4**: Na, 0.3 (0.31); P, 0.9 (0.8); Ru, 12.8 (11.0); W, 46.5 (47.6).

All elemental analyses were performed by Eurofins Umwelt West, Cologne, Germany. Infrared spectra for solid samples were obtained as KBr pellets on a Nicolet Avatar 370 FTIR spectrophotometer. Thermogravimetric analyses were performed on a TA Instrument SDT Q600 thermobalance with a 100 mL/min flow of nitrogen; the temperature was ramped from 20 to 800 °C/min at a rate of 5 °C/min. Samples were outgassed under a vacuum for 12 h using a Nova4000e (Quantachrome) instrument. Powder X-ray diffraction measurements were performed on a Siemens D5000 instrument using nickel-filtered Cu Kα radiation ($\lambda = 1.5418$ Å) from 3 to 38° θ with a step size of 0.010° and 10 s per step.

X-Ray Crystallography. Single crystals of compounds **1**−**4** were mounted in a Hampton cryoloop using light oil for data collection at low temperatures. Indexing and data collection were performed using a Bruker X8 APEX II CCD diffractometer with κ geometry and Mo Kα radiation ($\lambda = 0.71073$ Å). Data integration and routine processing were performed using the SAINT software suite. Further data processing, including absorption corrections from equivalent reflections, was performed using SADABS.[10] Direct methods (SHELXS97) solutions successfully located the W atoms, and successive Fourier syntheses (SHELXL97) revealed the remaining atoms.[11] Refinements were full-matrix least-squares against F^2 using all data. Cations and waters of hydration were modeled with varying degrees of occupancy, a common situation for polytungstate structures. In the final refinements, all nondisordered heavy atoms (W, K, Si, Ge, Mo, and Ru) were refined anisotropically, while the P and O atoms and some disordered cations were refined isotropically. Methyl H atoms were placed in calculated positions using a riding model. The crystallographic data for compounds **1**−**4** are summarized in Table 1.

Results and Discussion

Synthesis and Structure. Compound **1** was synthesized in an aqueous, acidic medium using a simple, one-pot procedure. The synthetic procedures for compounds **2**−**4** were similar to that of **1**, except that different polyanion precursors were used. All compounds **1**−**4** were characterized by single-crystal X-ray diffraction (XRD), FTIR spectroscopy, thermogravimetric analysis (TGA), and elemental analysis, while compound **1** was also investigated by powder X-ray diffraction. Unlike compounds **3** and **4**, which were synthesized using the plenary Keggin ($[\alpha\text{-}SiMo_{12}O_{40}]^{4-}$) or Wells-Dawson ($[\alpha\text{-}P_2W_{18}O_{62}]^{3-}$) polyanions, compounds **1** and **2** were prepared using the monolacunary undecatungstogermanate ($[\alpha\text{-}GeW_{11}O_{39}]^{8-}$) or -silicate ($[\alpha\text{-}SiW_{11}O_{39}]^{8-}$) polyanion precursors. It is evident that the rather low reaction pH of 2.0 resulted in the transformation of the lacunary $\{XW_{11}\}$ to the plenary $\{XW_{12}\}$ Keggin species. Compounds

(7) (a) Bilgrien, C.; Davis, S.; Drago, R. S. *J. Am. Chem. Soc.* **1987**, *109*, 3786. (b) Davis, S.; Drago, R. S. *Inorg. Chem.* **1988**, *27*, 4759.

(8) Some representative references: (a) Wilkinson, G.; Spencer, A. G. *J. Chem. Soc., Dalton Trans.* **1972**, 1570. (b) Sasaki, Y.; Tokiwa, A.; Ito, T. *J. Am. Chem. Soc.* **1987**, *109*, 6341. (c) Kikuchi, A.; Fukumoto, T.; Sasaki, Y.; Ichimura, A. *J. Chem. Soc., Chem. Commun.* **1995**, 2125. (d) Ota, K.; Sasaki, H.; Ito, T.; Kubiak, C. P. *Inorg. Chem.* **1999**, *38*, 4070. (e) Nunes, G. S.; Rocha, R. C.; Toma, H. E. *Eur. J. Inorg. Chem.* **2006**, 1487.

(9) (a) Haraguchi, N.; Okaue, Y.; Isobe, T.; Matsuda, Y. *Inorg. Chem.* **1994**, *33*, 1015. (b) Tézé, A.; Hervé, G. *Inorg. Synth.* **1990**, *27*, 89. (c) Sanches, C.; Livage, J.; Launay, J. P.; Fournier, M.; Jeannin, Y. *J. Am. Chem. Soc.* **1982**, *104*, 3194. (d) Contant, R. *Inorg. Synth.* **1990**, *27*, 105.

(10) *Siemens, SMART Users Manual*, version 4.050; Siemens Analytic X-ray Instruments: Madison, WI, 1996.

(11) Sheldrick, G. M. *SHELXTL*; Siemens Analytic X-ray Instruments: Madison, WI, 1993.

Table 1. Crystallographic Data for Compounds **1**−**4**

	1	**2**	**3**	**4**
emp formula	$C_{12}H_{84}GeK_2NaO_{86}Ru_3W_{12}$	$C_{12}H_{62}K_2O_{75}Ru_3SiW_{12}$	$C_{12}H_{53}K_2Mo_{12}O_{70}Ru_3Si$	$C_{36}H_{125.4}K_{1.5}Na_{0.25}O_{136.7}P_2Ru_9W_{18}$
fw	4288.0	4022.3	2878.3	7091.2
cryst syst	monoclinic	monoclinic	monoclinic	monoclinic
space group	$P2_1/n$	$P2_1/n$	$P2_1/n$	$P2_1/n$
a (Å)	14.3538(5)	15.4993(5)	14.4232(9)	17.7646(6)
b (Å)	18.0407(5)	18.0110(5)	17.9103(7)	29.5710(12)
c (Å)	31.8655(10)	29.4804(7)	31.6511(18)	29.7274(10)
β (deg)	100.472(2)	93.184(2)	99.990(3)	91.748(2)
vol (Å^3)	8114.2(4)	8217.0(4)	8052.3(7)	15609.0(10)
Z	4	4	4	4
temp (°C)	−100	−100	−100	−100
d_{calcd} (mg/m^3)	3.510	3.251	2.374	3.018
abs coeff (mm^{-1})	18.077	17.483	2.572	14.220
R $[I > 2\sigma(I)]^a$	0.052	0.050	0.081	0.062
R_w (all data)^b	0.150	0.160	0.243	0.163

^{a} $R = \sum||F_o| - |F_c||/\sum|F_o|$. ^{b} $R_w = \sum_w(F_o^2 - F_c^2)^2/\sum_w(F_o^2)^2]^{1/2}$.

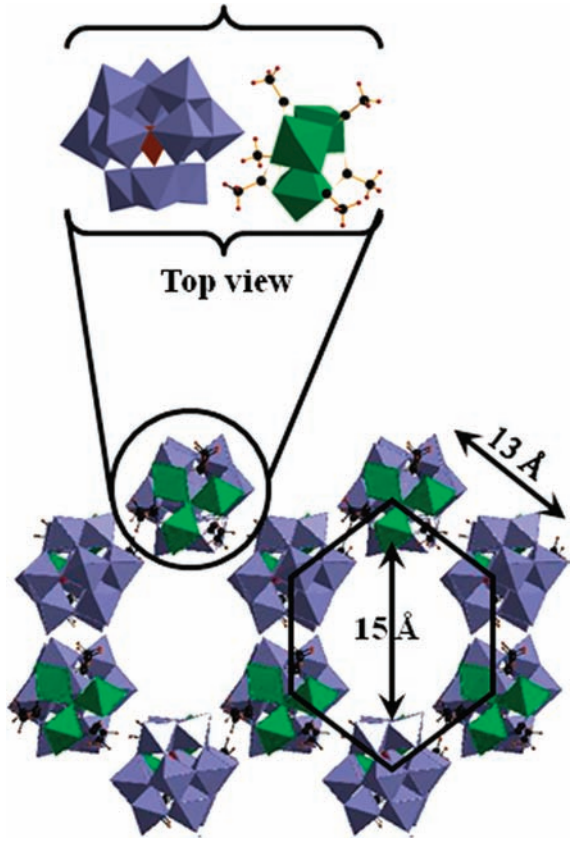

Figure 1. Top: Ball-and-stick/polyhedral presentation of **1**. The color code is as follows: WO_6 (blue), GeO_4 (dark red), RuO_6 (green), carbon (black), and hydrogen (brown). Bottom: view of the solid state packing of **1** along the *b* axis showing the hexagonal channels with a depth of about 16 layers. Potassium/sodium ions and crystal waters not shown for clarity.

1−**3** are isostructural, and they all crystallize in the monoclinic space group $P2_1/n$ either as a mixed potassium/sodium salt (**1**) or as a potassium salt (**2**, **3**). Figure 1 shows the arrangement of the anionic $\{GeW_{12}O_{40}\}$ units and the cationic $[Ru_3O(OOCCH_3)_6(OH_2)_3]^+$ (**Ru_3**) in the solid state. The crystal packing of **1** reveals hexagonal channels along the *b* axis of the unit cell. These hexagonal channels are formed from parallel, alternating polyanion/**Ru_3** rows, arranged so that at each corner of the hexagonal channel there are also alternating polyanion/**Ru_3** positions. Therefore, each "section" of the hexagonal channels contains alternatingly three polyanion and three **Ru_3** molecules (see Figure 1).

The idealized symmetry of the channels reveals regular hexagons with an edge length of about 13 Å. Structural data show a channel diameter of ca. 15 Å. Interestingly, these channels are occupied with crystal waters, most of which are weakly coordinated to the K^+/Na^+ counter cations, which in turn are coordinated to oxygens of the polyanions and **Ru_3** in the vicinity of the channels (close to the hexagonal edges). Keeping this in mind, removal of the water molecules by heating might result in "empty channels", which can offer potential sorption properties. The absence of counter cations inside the channels reinforces such possibilities.

This is why we treated compound **1** under different outgassing conditions (100 and 150 °C under a vacuum), then allowed the samples to cool down to room temperature under inert gas (N_2), followed by TGA. All of these results are compared with the non-pretreated sample **1** (vide infra).

Compound **4** crystallizes as a mixed sodium−potassium salt in the monoclinic space group $P2_1/n$. In the solid-state structure of **4**, each $[\alpha\text{-}P_2W_{18}O_{62}]^{6-}$ polyanion is surrounded by three **Ru_3** units, resulting in a macrocation/macroanion assembly with a total charge of −3, in complete analogy with **1**−**3** (see Figure 2). The crystal packing of **4** along the *b* axis also involves hexagonal arrangements of two main types of columns, which we identify as A and B. Column A corresponds to **Ru_3** units, whereas column B corresponds to alternating $[\alpha\text{-}P_2W_{18}O_{62}]^{6-}$/**$Ru_3$** units. The third column, C, also corresponding to alternating $[\alpha\text{-}P_2W_{18}O_{62}]^{6-}$/**$Ru_3$** units but reversed with respect to column B, is centered with respect to each hexagonal arrangement of columns A and B (see Figure 2 for more details).

The IR spectra (Figures S5−S8 in the Supporting Information) of compounds **1**−**4** all show two separate ranges of bands. The fingerprint region for the respective Keggin and Wells-Dawson polyanions is observed between 400 and 1200 cm^{-1}, whereas the bands for **Ru_3** can be identified in the range 1300−1650 cm^{-1}. The fact that the IR spectra of **1**−**4** are essentially the sum of the spectra of the two components (polyanion + trinuclear cation) reflects the absence of covalent intermolecular interactions. It appears that electrostatic and packing forces mainly hold together the polyanions and **Ru_3** cations in our products **1**−**4**. Such intermolecular interaction reduces the charge of the macrocation/macroanion

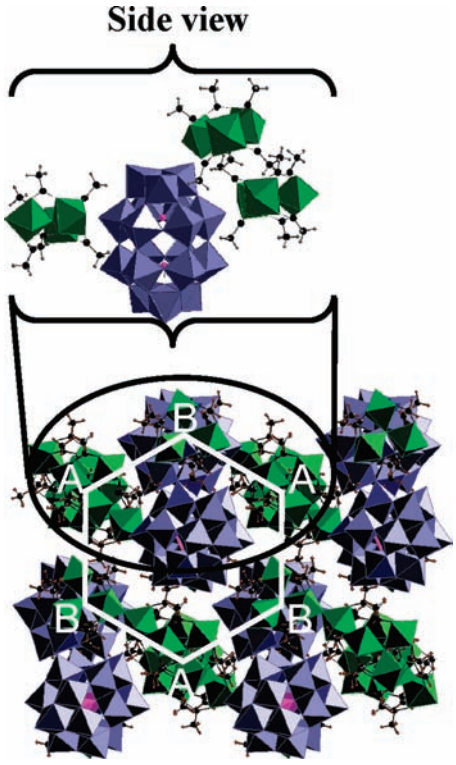

Figure 2. Top: Ball-and-stick/polyhedral presentation of **4**. The color code is the same as in Figure 1, with purple tetrahedra, PO_4. Bottom: view of the solid state packing of **4** along the *b* axis showing the hexagonal channels with a depth of about 16 layers. Potassium/sodium ions and crystal waters not shown for clarity.

assemblies to −3 for all materials **1**−**4**. This remaining charge is balanced in the solid state by potassium or sodium counter cations, which are located in the interstices. It is not surprising that the larger Wells-Dawson ion, compared to the Keggin ion, is surrounded by three rather than one $\mathbf{Ru_3}$.

TGA for **1**−**4** indicated very similar behavior for all four compounds (see Figures S1−S4, Supporting Information). The thermogravimetric profiles show the occurrence of dehydration followed by decomposition in two main steps. The dehydration process involves the release of crystal waters. The TGA weight loss of ∼5% up to 200 °C for compound **1** can be assigned to ∼10 H_2O's, which corresponds exactly to the formula unit of **1** (vide supra). The weight loss occurs in two steps, with the first step up to 100 °C corresponding to ∼3% (∼6 H_2O's, loosely bound water) and the second step between 100 and 200 °C corresponding to ∼2% (∼4 H_2O's, tightly bound water). A sharp weight loss around ∼300−350 °C is observed due to decomposition of the macrocation $\mathbf{Ru_3}$. The thermograms of **2**−**4** are similar to that of **1**, exhibiting a loss of crystal water up to ca. 200 °C followed by decomposition starting at ca. 300 °C (see Supporting Information).

Sorption Studies. Due to the particularly interesting solid-state structure of **1**, exhibiting large channels filled with crystal waters, we decided to perform sorption studies on this compound. These studies involved outgassing samples under a vacuum at different temperatures and checking for water content by TGA. Powder XRD measurements were also performed on the outgassed samples and compared with those of the hydrated ones. As TGA for compound **1** showed two water loss steps, we decided to test if the loosely and tightly bound waters could be selectively outgassed.

If compound **1** is initially outgassed at 150 °C followed by TGA on this sample, no water loss is observed, indicating that it had disappeared already (see Figure 3). However, if the outgassing on **1** is performed at 100 °C under a vacuum followed by TGA on this sample, then a weight loss of ∼2% (∼4 H_2O's) was observed (see Figure 3). This indicates total lattice water removal at 150 °C without a vacuum versus selective removal of only the loosely bound crystal waters at 100 °C under a vacuum. Powder XRD measurements on a sample of **1** which had been outgassed at 150 °C showed essentially the same peak pattern as for the hydrated form, but with a slight shift toward lower angles reflecting a small change in the unit cell dimensions (see Figure 4). This indicates that dehydration of compound **1** does not affect its crystalline nature and essentially does not alters its solid-state packing arrangement.

Interestingly, if compound **1** is outgassed at 150 °C under a vacuum and then exposed to ambient air for 48 h, its TGA changes and becomes virtually identical with that of the hydrated form (see Figure 3). Furthermore, XRD measurements showed that the air-exposed sample had the same powder pattern as that of the original sample (see Figure 5). Therefore, compound **1** can lose and regain its crystal water molecules without changing crystalline order. Our preliminary outgassing studies on **2** indicate that this material has a very similar behavior to that of **1**. We expect the same for **3**, due to the isostructural nature of **1**−**3**. On the other hand, the solid-state structure of **4** is completely different from that of **1**−**3**, as the former does not exhibit any channels in the solid state (see Figure 2). Our preliminary thermal, powder XRD, and outgassing studies on **4** have shown that this material does not undergo a reversible loss of crystal waters. In fact, the crystallinity of **4** is completely lost upon heating to 150 °C.

We also decided to investigate the sorption properties of compound **1** with different short-chain alcohols, namely, methanol and ethanol. Compound **1** was pretreated under a vacuum at 150 °C to remove all crystal water molecules and was then immersed in 1 mL of methanol or ethanol and kept in an open vial until complete evaporation of the liquid was achieved. Afterward, TGA measurements were performed on the remaining solids (see Figure 6). The TGA graph for the ethanol-treated sample showed less weight loss than that with methanol, indicating less sorption of ethanol than methanol. Furthermore, the methanol-treated sample showed a sharper slope for the first weight loss step, which may reflect the lower boiling point of methanol as compared to ethanol.

The powder XRD measurements on samples of **1** after alcohol adsorption showed a loss of crystallinity, as identified by the absence of any distinguishable peaks. Then, the same samples were outgassed at 150 °C and investigated by powder XRD. However, the results showed that the powders were not crystalline and were different from the original

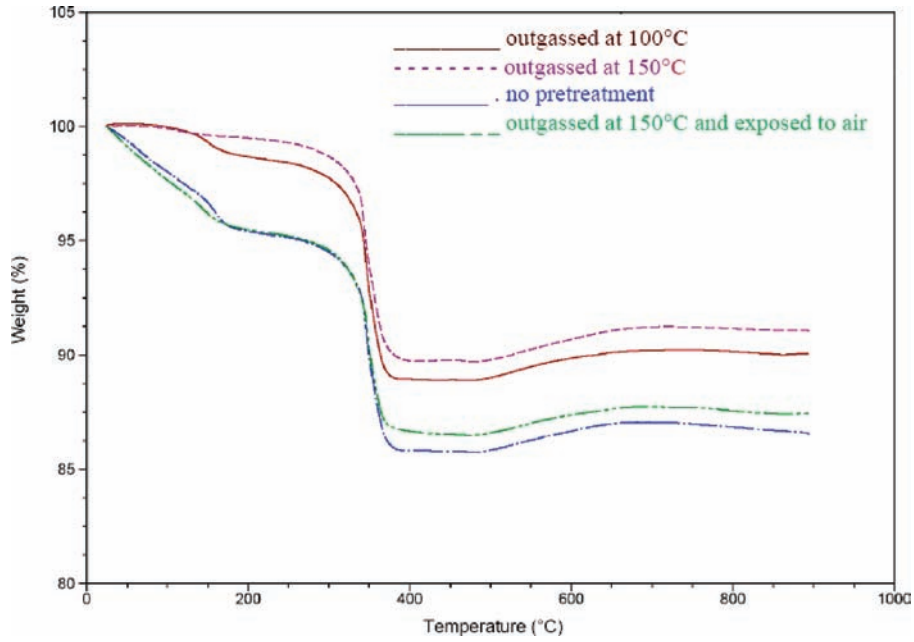

Figure 3. Thermogram of **1** without any pretreatment (blue), outgassed under a vacuum at 150 °C (purple), outgassed under a vacuum at 100 °C (red), and exposed to air for 48 h after outgassing at 150 °C (green).

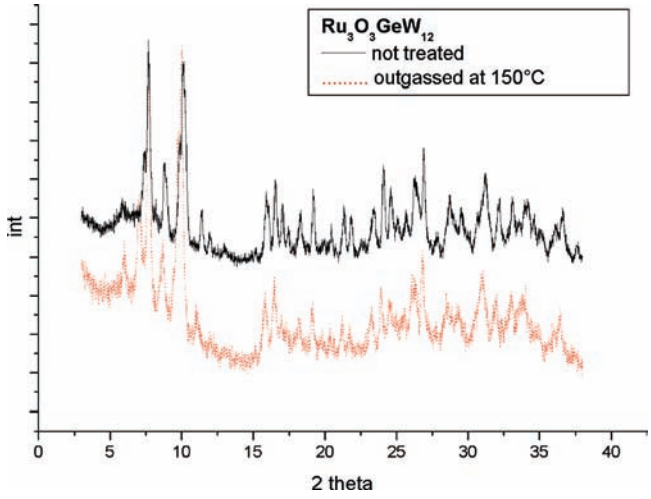

Figure 4. Powder XRD pattern of compound **1** outgassed at 150 °C under a vacuum (black) and without any pretreatment (red).

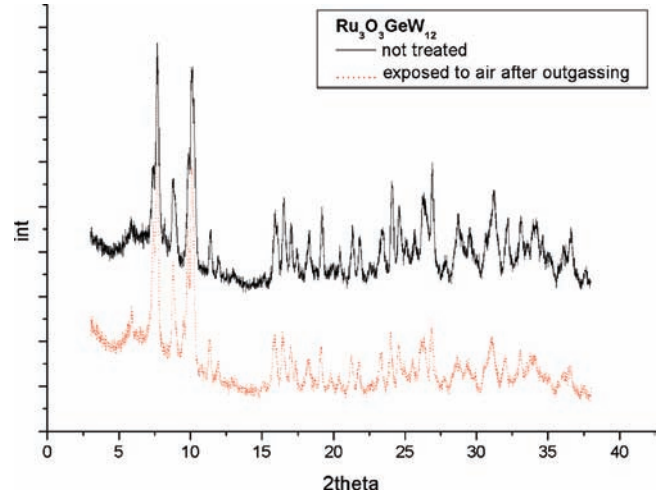

Figure 5. Powder XRD pattern of compound **1** exposed to air for 48 h after outgassing at 150 °C under a vacuum (red) and without any pretreatment (black).

outgassed material. We conclude that the alcohol sorption with **1** is irreversible and may in fact lead to a change in the solid-state packing of the material.

To investigate in more detail the solid-state modifications of **1** after exposure to ethanol and methanol, TGA measurements on outgassed samples after exposure to the alcohol were also performed (see Figure 6). The curve depicting the TGA of outgassed **1** after exposure to ethanol (pink line) is not superimposable with the one of the originally outgassed sample (black line). This suggests a solid-state rearrangement of **1** upon interaction with the ethanol molecules. The graph of the sample outgassed after exposure to methanol (green line) showed an even more different behavior with a drawn out weight loss step ranging from about 300 to 600 °C. The fact that **1** adsorbs a larger quantity of methanol than ethanol (red vs blue curve) may suggest that methanol (perhaps due to its smaller size) penetrates deeper into the channels of **1** as compared to ethanol, thus affecting the solid-state packing more. We believe that the featureless weight loss between 300 and 600 °C could be due to methanol molecules deep in the channels and hydrogen bonded to the trinuclear ruthenium cations and POM anions. However, more detailed sorption studies using other (less polar) organic molecules are needed to confirm this hypothesis.

Conclusions

We have investigated for the first time the interaction of the trinuclear, oxo-centered ruthenium(III) cation $[Ru_3O(OOCCH_3)_6(H_2O)_3]^+$ with Keggin and Wells-Dawson polyanions in an aqueous solution. This work has resulted in the synthesis of the four compounds **1**−**4**, which crystallize as potassium or mixed potassium/sodium salts and which have been fully characterized in the solid state by single-crystal XRD, FTIR, TGA, and elemental analsyis. The Keggin-based systems **1**−**3** exhibit hexagonal channels in the solid-state lattices

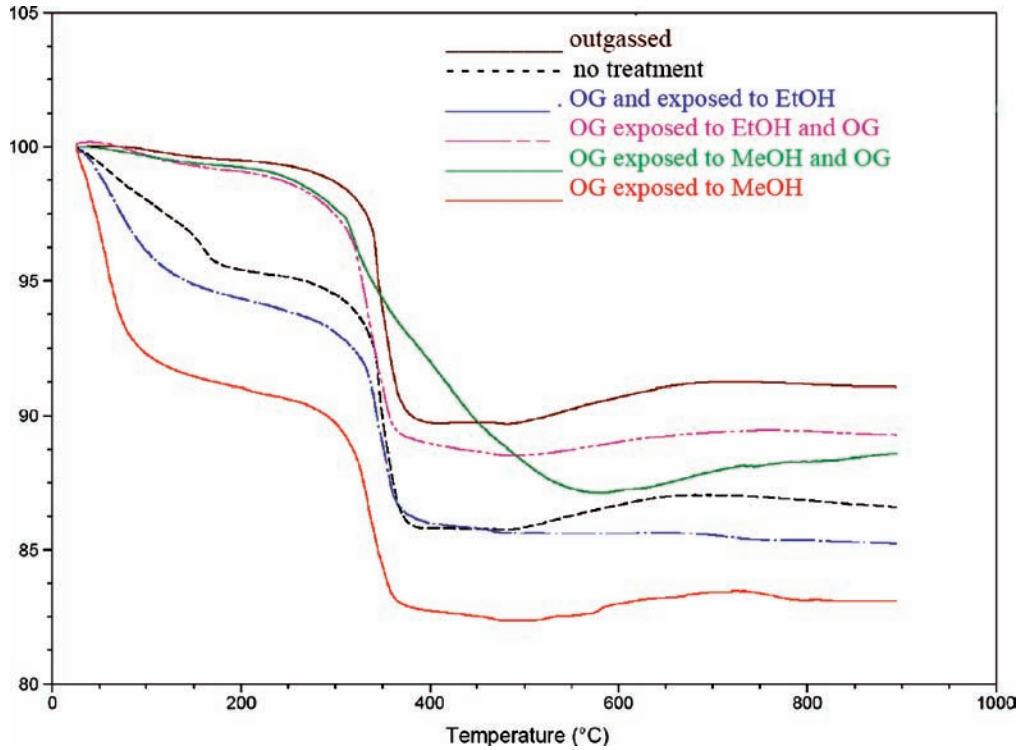

Figure 6. Thermogram of **1** without any pretreatment (black), outgassed under a vacuum at 150 °C (brown), outgassed exposed to methanol (red) and outgassed again (green), and outgassed then exposed to ethanol (blue) and outgassed again (pink).

which are filled with crystal waters, indicating a potential for interesting sorption properties. Sorption/desorption studies on **1** for water indicated reversible behavior, as seen by powder-XRD and TGA. On the other hand, the same studies on **1** for methanol and ethanol as well as for mixtures of the two alcohols indicated irreversibility due to decomposition of **1**. The solid-state structure of **4** does not exhibit any channels in the solid state, and as expected, our preliminary thermal, powder XRD, and outgassing studies showed that this material does not undergo a reversible loss of crystal waters.

In future work, we plan more detailed sorption studies using other molecules which are less polar than methanol and ethanol. Furthermore, heterogeneous oxidation catalysis studies making use of the coexistence of redox-active Ru^{3+} and polytungstates and -molybdates in the same material and in close proximity are planned. We will also explore whether in situ decomposition of the trinuclear Ru precursor can result in novel Ru-containing polyanions. In addition, we plan to investigate the interaction of other metal derivatives of $\mathbf{Ru_3O}$ (e.g., Pt, Rh, Ir, Fe, and Mn) with lacunary and plenary polyanions.

Acknowledgment. U.K. thanks Jacobs University and the Fonds der Chemischen Industrie for research support. M.I. thanks DAAD and the Higher Education Commission of Pakistan for a doctoral fellowship, as well as Dr. Sib Sankar Mal for assistance in the laboratory and Dr. Bassem Bassil for help with the preparation of this manuscript. Figures 1 and 2 were generated using Diamond, version 3.1f (copyright Crystal Impact GbR).

Supporting Information Available: Thermograms, FTIR spectra, and X-ray crystallographic data (CIF) for **1**−**4**. This material is available free of charge via the Internet at http://pubs.acs.org.

IC802096V